Energy 76 (2014) 428–435

Contents lists available at ScienceDirect

Energy

journal homepage: www.elsevier.com/locate/energy

Flow boiling heat transfer on nanowire-coated surfaces with highly wetting liquid

Sangwoo Shin [1], Geehong Choi [1], Beom Seok Kim, Hyung Hee Cho*

Department of Mechanical Engineering, Yonsei University, Seoul 120-749, South Korea

ARTICLE INFO

Article history:
Received 18 February 2014
Received in revised form
28 July 2014
Accepted 9 August 2014
Available online 15 September 2014

Keywords:
Boiling heat transfer
Forced convection
Nanowire
Wetting
Bubble nucleation

ABSTRACT

Owing to the recent advances in nanotechnology, one significant progress in energy technology is increased cooling ability. It has recently been shown that nanowires can improve pool boiling heat transfer due to the unique features such as enhanced wetting and enlarged nucleation sites. Applying such nanowires on a flow boiling, which is another major class of boiling phenomenon that is associated with forced convection, is yet immature and scarce despite its importance in various applications such as liquid cooling of energy, electronics and refrigeration systems. Here, we investigate flow boiling heat transfer on surfaces that are coated with SiNWs (silicon nanowires). Also, we use highly-wetting dielectric liquid, FC-72, as a working fluid. An interesting wetting behavior is observed where the presence of SiNWs reduces wetting and wicking that in turn leads to significant decrease of CHF (critical heat flux) compared to the plain surface, which opposes the current consensus. Also, the effects of nanowire length and Reynolds number on the boiling heat transfer are shown to be highly non-monotonic. We attempt to explain such an unusual behavior on the basis of wetting, nucleation and forced convection, and we show that such factors are highly coupled in a way that lead to unusual behavior.

1. Introduction

Boiling is one representative mode of phase-change phenomenon between liquid and vapor that is associated in a great part of our life due to its universality. In particular, large latent heat of vaporization can enable efficient cooling under extreme thermal conditions in energy systems and integrated circuits, so vast studies on applications as well as fundamentals of boiling heat transfer were extensively conducted during the past several decades [1]. Recently, with aid of nanotechnology, it has been revealed that nanomaterials can significantly enhance boiling heat transfer performance. Especially, surfaces with 1-D nanomaterials, i.e. nanowires, were shown to enhance CHF (critical heat flux) up to 100% compared to the plain surface, which can increase the safe margin under extreme thermal conditions [2]. Such nanowire-coated surfaces were believed to enhance boiling heat transfer due to several unique features such as increased number of nucleation sites, enhanced wetting, capillary pumping and increased surface area [2].

The majority of such studies were investigated under pool boiling condition where the working fluid is stagnant [2–7]. In contrast, studies regarding nanomaterials on a flow boiling, which is another major class of boiling phenomenon that is associated with forced convection, are yet immature and scarce despite its importance in various applications such as liquid cooling of nuclear reactors and highly-integrated electronics as well as phase-change components in refrigeration systems. Very recently, Li et al. have studied flow boiling with SiNWs (silicon nanowires) using water as a working fluid and showed that SiNWs can also enhance heat transfer performance and stabilize pressure fluctuation under flow boiling condition [8]. Also, Morshed et al. have investigated similar experiment on flow boiling with water using electrodeposited copper nanowires, which exhibit similar morphology with SiNWs [9]. They also observed that the nanowires were beneficial to heat transfer coefficient.

Regarding that such recent studies are conducted using water, only limited studies have been conducted with dielectric liquid and still remains unclear, which is also an important issue on flow boiling, especially in cooling of electronics [10]. Because dielectric liquids are mostly non-polar, thereby having low surface tension with high wettability [11], it is anticipated that the dielectric liquids will show an interesting boiling behavior compared to water.

* Corresponding author.
E-mail address: hhcho@yonsei.ac.kr (H.H. Cho).
[1] These authors contributed equally to this work.

http://dx.doi.org/10.1016/j.energy.2014.08.037
0360-5442/

Here, we investigate flow boiling heat transfer on SiNWs-coated surface using dielectric liquid. We employ FC-72 as a dielectric liquid, which is a highly wetting liquid with low surface tension (12 mN/m at 25 °C) and low viscosity (0.64 mPa s at 25 °C) compared to deionized water [12]. We study effects of various SiNWs and Reynolds number on boiling heat transfer performance, and unlike water, we observe an interesting behavior of boiling performance in terms of CHF and HTC (heat transfer coefficient) when highly wetting liquid is used. We show that convective heat transfer also plays a major role in heat transfer along with nucleation cavities. We attempt to explain this complex behavior by investigating interactions between wetting, nucleation cavities and forced convection.

2. Experimental details

2.1. Microfabricated heater/sensor unit

In order to apply heat flux and measure wall temperature simultaneously, we made a heater/sensor unit via microfabrication techniques (Fig. 1a). Platinum with thickness of 100 nm was patterned on a double side-polished silicon substrate for use as a RTD (resistance temperature detector) for measuring temperature, followed by patterning 800 nm-thick ITO (indium tin oxide) layer, which serves as a thin film heater. Between these two layers, an insulation layer ($SiO_2/Si_3N_4/SiO_2$) was deposited. For stable supply of electric current to the ITO heater, a thin layer of copper followed by gold was partially deposited on the electrode parts of ITO layer.

2.2. Nanowire synthesis

On the backside of the silicon substrate, SiNWs were synthesized on an area of 14 × 8 mm^2 where the longer side is parallel to the streamwise direction (Fig. 1b). For SiNWs synthesis, metal-assisted chemical etching method was employed. Initially, surface was cleaned with piranha solution (H_2O_2:H_2SO_4 = 1:3 v/v) for 40 min to remove organic materials, then cleaned with acetone followed by methanol. After cleaning, the wafer was immersed in 5 mM $AgNO_3$ and 4.8 M HF solution for 1 min in order to reduce silver ions on the surface of the silicon substrate. After cleaning with deionized water, substrate was dipped in the solution of 4.8 M HF and 0.1 M H_2O_2 for silver-assisted chemical etching. Reduced silver nanoparticle acts as a cathode at the interface between the etching solution and the silicon substrate, and H_2O_2 was reduced to water. Holes, which were generated from the cathode, were injected to the interface between silver particles and silicon substrate. In this way, silicon substrate was oxidized with holes and subsequently etched by HF solution. With this process, the silicon substrate can be etched down straightly with extreme aspect ratio and form uniform nanowires on the surface [13–15].

2.3. Flow boiling setup

The test section, shown in Fig. 1c, consists of top and bottom part that can be assembled to form a flow channel. The top and bottom parts were made of acrylic except for the transparent window near the heater area for visualization, which was made of quartz to endure high temperature. The RTD-array sensors were located on top of an insulator (polyetheretherketone, PEEK), which has holes for access to the electrical wirings for the sensors and the heater. Glass transition temperature of PEEK is around 143 °C, so a stable experiment could be performed. The heating current was supplied to the ITO heater through copper busbars, and the following voltage drop was measured to calculate the generated heat.

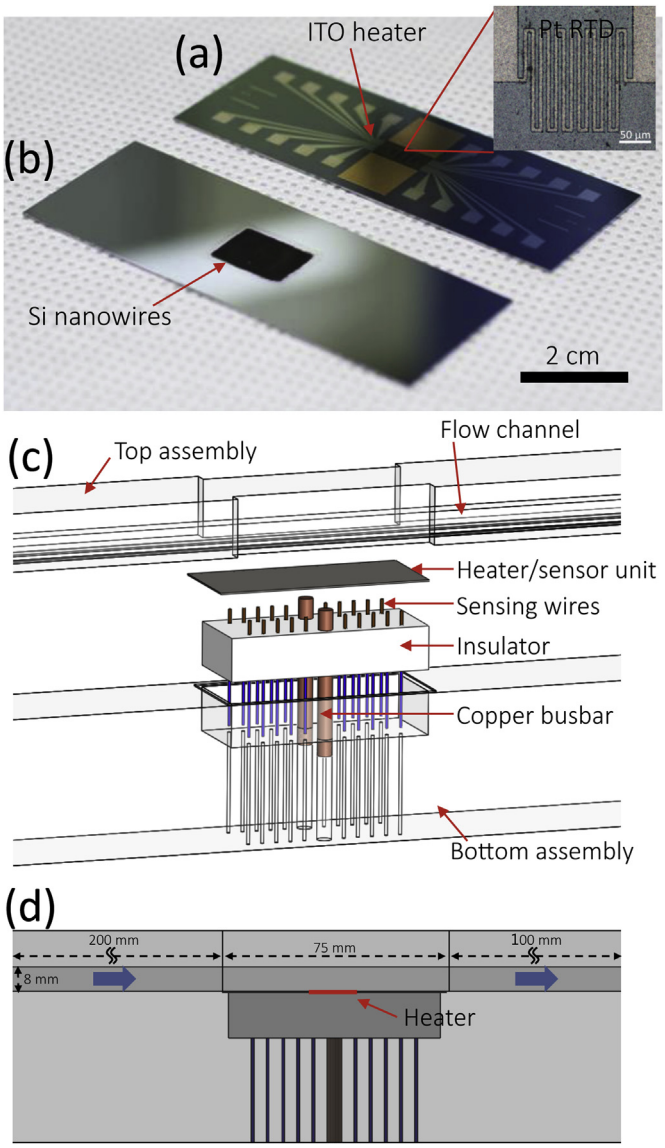

Fig. 1. Experimental setup. Optical images of (a) Microfabricated heater/sensor unit with platinum RTD sensor (inset) and (b) SiNWs on the backside of the unit. (c) Schematic of the test section for flow boiling. (d) Cross-section of the test section.

The cross-sectional area of the main channel was 8 × 8 mm^2 and the channel length was long enough to ensure the fully developed condition of the mainflow [16]. The test loop was a closed-loop configuration. The working fluid was FC-72 (3M, USA) and was contained in the main reservoir. The main reservoir was connected to an additional chamber to control the pressure. A magnetic pump (TXS5.3, Tuthil Co., CA, USA) and a three-phase motor (0.5 HP, 3500 rpm, LG-OTIS, Korea) drove the working fluid to a mass flow meter (ULTRA-mass MK II, Oval Co.), which measured the flow rate. The temperature of the flow stream was controlled by a heat exchanger (Flatplate, Model 131001694), which is able to maintain the temperature of the working fluid within 1 °C of deviation. Prior to experiment, working fluid was degassed by heating the working fluid up to the boiling point with an immersion heater for 2 h while running the test loop. J-type thermocouple (Omega, USA.) and pressure gauge (PMP 4070 for absolute pressure, PMP4170 for differential pressure, GE Druck, USA.) were employed to continuously monitor the temperature

and pressure change of the working fluid, respectively, at the both ends of the channel. Bubbles during nucleate boiling were visualized with high-speed camera (pco.4000, PCO, Germany). The experiments were operated under the saturation temperature of FC-72, which is 56 °C at atmospheric pressure.

3. Results and discussion

To seek for the combined effect of nanowires and forced convection on boiling heat transfer performance, we coated SiNWs on one side of the channel wall via metal-assisted chemical etching method [13–15], while backside of the nanowire-coated surface being heater and temperature sensor. Fig. 2a–c shows SEM (scanning electron microscope) images of the fabricated SiNWs with various lengths, which range from 0.8 μm to 15.7 μm depending on the etching time. Also, due to the agglomeration of the nanowires during the wet chemical processes, microscale cavities were naturally formed (Fig. 2d–f), which is regarded as one of the most important features that favors boiling heat transfer [2,3]. In addition, the size of such cavities tends to increase with nanowire length, and the range becomes broader (Fig. 2g), as quantitatively analyzed by digital image analyzer.

Unlike other major flow boiling studies where the streamwise bubble structure evolution is studied [17], this study focuses on the heat transfer performance, i.e. CHF and HTC. Thus, relatively a short heater is employed instead of a long heater that spans over the entire channel wall [18]. This feature additionally gives negligible pressure drop due to the presence of nanowires, which was measured to be below the detectable range of the pressure transducer. Also, flow channel with relatively large cross-section was employed compared to the nanowire length where CHF is occurred prior to channel blockage with vapor columns and films. So in this study, CHF is considered as an instantaneous wall temperature jump where the term is normally defined in the pool boiling experiments, rather than blockage of the channel by vapors, which is commonly observed in microchannel flow boiling experiments [8].

Employing these nanowire-coated surfaces to flow boiling experiments with FC-72, we obtained the boiling curves under various Reynolds number as shown in Fig. 3. The results raise two interesting points: First, CHF is much lower when nanowires are employed, regardless of the nanowire length. Second, nanowire length and Reynolds number dependence on HTC is highly non-monotonic. In the following section, we attempt to explain such unusual behaviors on the basis of complex interactions between surface wetting, nucleation, and convective heat transfer.

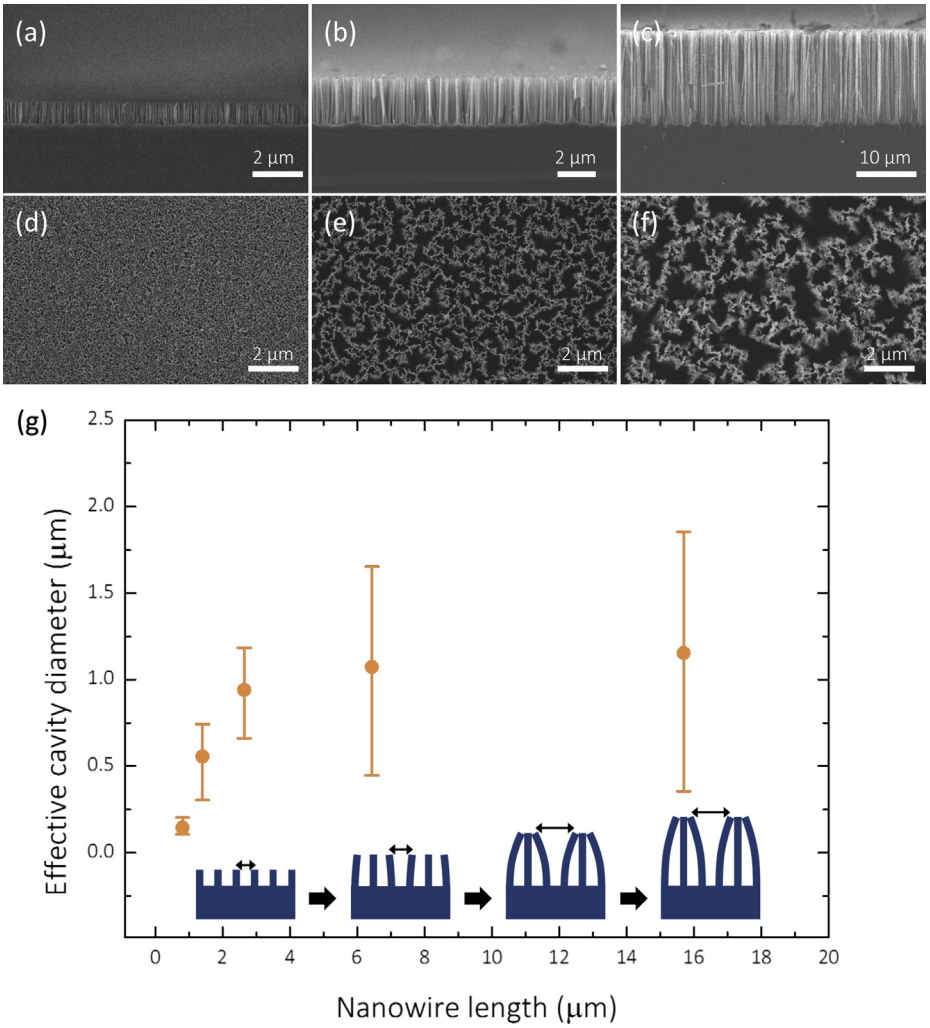

Fig. 2. Synthesized SiNWs with various lengths. SEM images of the (a)–(c) cross-section and (d)–(f) top view of SiNWs with various lengths; (a), (d) Nanowire length of 0.8 μm; (b), (e) Nanowire length of 2.6 μm; (c), (f) Nanowire length of 15.7 μm. (g) Effective cavity diameter vs. nanowire length. The error bars represent the size range of the observable cavities. Inset is an illustration depicting the cavity size change as the nanowire length increases.

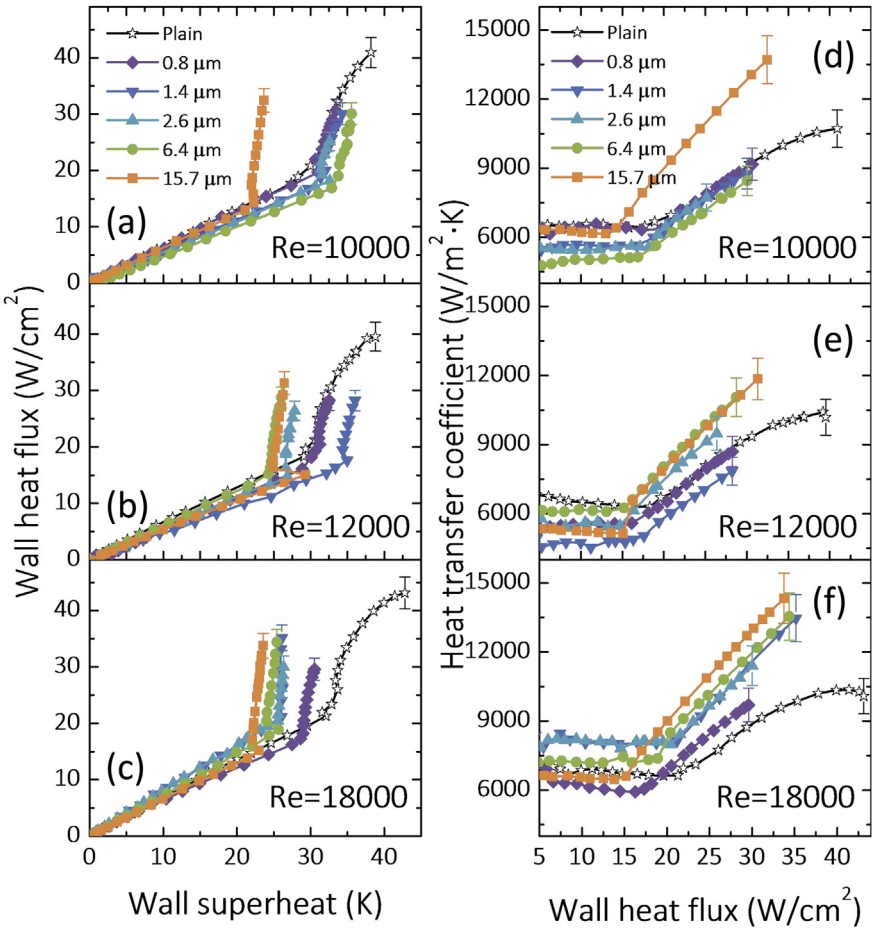

Fig. 3. Boiling curves. (a)–(c) Wall heat flux vs. wall superheat under various nanowire lengths and Reynolds numbers. (a) *Re* = 10,000 (velocity = 34.3 cm/s, mass flow rate = 2.1 kg/s); (b) *Re* = 12,000 (velocity = 41.2 cm/s, mass flow rate = 2.52 kg/s); (c) *Re* = 18,000 (velocity = 61.8 cm/s, mass flow rate = 3.78 kg/s); (d)–(f) Heat transfer coefficients vs. wall heat flux under various nanowire lengths and Reynolds numbers. (d) *Re* = 10,000; (e) *Re* = 12,000; (f) *Re* = 18,000.

3.1. Critical heat flux

As we look into CHF first, CHF value has marked around 40 W/cm^2 for the plain surface whereas it was shown to be around 30 W/cm^2 for the nanowire-coated surfaces, regardless of the nanowire length. It is generally known that the nanowires greatly enhance the surface wettability and also promote the capillary pumping which increases CHF for over 100% compared to the plain surface [2]. Also, in a recent study by Li et al. has shown that SiNWs can enhance CHF in flow boiling when water is used as a working fluid [8]. Despite these facts that SiNWs are favorable for CHF regardless of the forced convection, our results clearly show that the SiNWs significantly degrades CHF.

One well-known factor that governs CHF is wettability [19,20]. In this regard, we first measured contact angles of the nanowire-coated surfaces with FC-72 and compared with deionized water. As shown in Fig. 4a, we observed an interesting behavior such that the presence of nanowires actually reduces wettability (contact angle increase) of FC-72 in contrast to water. In particular, the contact angle was decreased from 43.6° (plain) to 4.5° (15.7 μm-long SiNWs) for water whereas it was unambiguously increased from 9.8° (plain) to 16.1° (15.7 μm-long SiNWs) for FC-72. Moreover, the contact angle tends to increase slightly as the nanowire length increases, i.e. roughness increases. This directly opposes the Wenzel relation in hydrophilic regime, where it states that the roughness favors wettability [21,22]. Such an observed behavior is not fully understood at this point and requires further study, but one possible reason that we attribute is due to the weak hemi-wicking of the FC-72 inside the nanowires [22]. Due to the high viscosity to surface tension ratio of FC-72 compared to water (about four times larger at room temperature), capillary wicking is suppressed, which can be verified in Fig. 4b and c where the front line of the precursor film cannot be observed in FC-72, whereas that of the water is clearly seen. This should lead to the formation of local air pockets among the nanowires that reside beneath the droplet, which should result in increased contact angle. Moreover, the droplet is firmly pinned for water whereas FC-72 droplet is unstable accompanied with fast evaporation due to large vapor pressure (~30 kPa at 25 °C), which implies a quasi-Cassie-Baxter-like behavior [23]. Therefore, due to the reduced wetting and suppressed capillary pumping of FC-72, the CHF of the nanowire-coated surface is significantly reduced compared to the plain surface.

One more possible reason that we attribute to the lowered CHF of the nanowire-coated surface is the blockage of the mainflow momentum, which hinders from disturbing the vapor layer. By definition, CHF occurs as the heated surface is fully covered with vapor film that does not allow for the surface to be in a direct contact with the liquid. On the plain surface, the mainflow momentum can push away such a vapor film, which effectively extends CHF. However, on the nanowire-coated surface, the vapor layer is formed within the nanowires. Thus, vapor film removal by

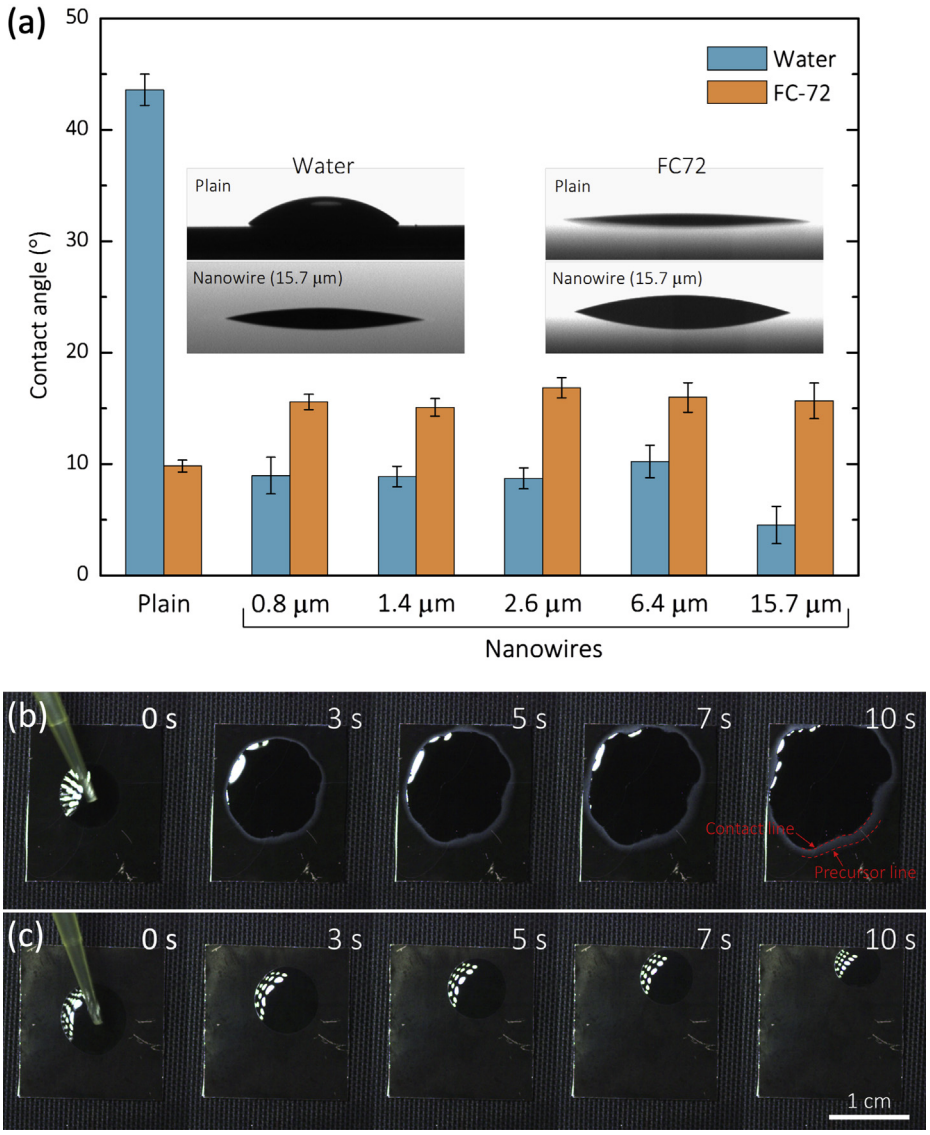

Fig. 4. Wetting experiments. (a) Measured contact angles of nanowires with various length for water (orange) and FC-72 (blue). Insets are contact angle images for plain and nanowire (length = 15.7 μm) surfaces with water and FC-72. (b), (c) Time-dependent wicking test for nanowire surface (length = 15.7 μm) with (b) water and (c) FC-72. The front line of precursor film is clearly observed for water whereas it is not for FC-72. (For interpretation of the references to color in this figure legend, the reader is referred to the web version of this article.)

the mainflow cannot be expected for the nanowire-coated surfaces. Furthermore, a direct disturbance of the vapor layer by nanowires in this study cannot be expected, as previously shown by long and dense carbon nanotube arrays [24]. This is because the thickness of the vapor layer for FC-72 is known to be typically around 15–20 μm [24], which is larger than the length of the nanowires in this study. Therefore, reduced wetting/wicking as well as hindered vapor film disturbance are believed to be the possible reasons for the lowered CHF.

3.2. Single-phase heat transfer coefficient

Besides CHF, another important factor that defines the efficacy of boiling performance is HTC. From the boiling curve, HTC can be estimated from the ratio of the wall heat flux to the wall superheat, on the basis of Newton's law of cooling. The results are presented in Fig. 3d–f, and it shows nonmonotonic behavior.

Observing the single-phase region first, HTC is constant throughout the heat flux, but highly nonmonotonic with respect to the nanowire length as well as Reynolds number. Fig. 5a shows HTC at 10 W/cm^2 vs. nanowire length for a clear view. Although the behavior is nonmonotonic, the trend over the entire Reynolds numbers is somewhat similar: HTC decreases to a certain point, then rapidly increases, followed by gradual decrease again. The point where HTC reaches minimum is shown to decrease with Reynolds number, which is marked with red arrows.

Under single-phase condition, the length of nanowires affects the geometry of the surface (insets in Fig. 2g) whereas the Reynolds number affects the fluid momentum. Initially, the nanowires act as a local barrier that reduces the mainflow momentum that can penetrate into the bottom surface of the nanowires, thus reducing heat transfer. This should be pronounced in this study because the nanowires are located just below the channel surface owing to the fabrication mechanism of nanowires, where the nanowires are formed by 'etching down' the silicon substrate. This is the reason

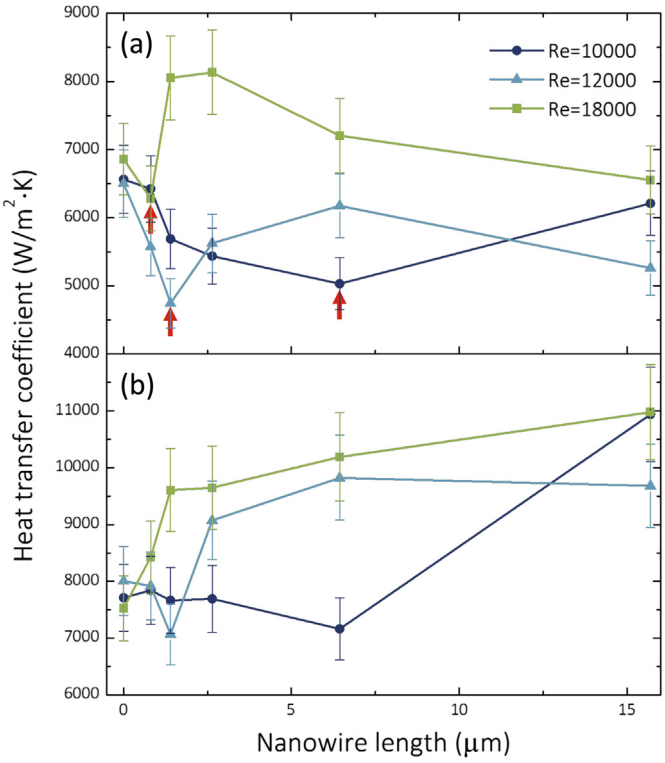

Fig. 5. Heat transfer coefficients vs. nanowire length obtained at constant wall heat flux of (a) 10 W/cm^2 and (b) 25 W/cm^2. Red arrows in (a) indicate critical nanowire lengths. (For interpretation of the references to color in this figure legend, the reader is referred to the web version of this article.)

why HTC initially decreases as the nanowire length increases. Especially, at the low Reynolds numbers (Re = 10,000 and 12,000), HTC of the plain surface is shown to be higher than any other nanowire-coated surfaces because the mainflow does not carry enough momentum to penetrate into the bottom surface for nanowire-coated surfaces whereas it can be directly transferred onto the heating surface for the plain surface.

However, as the nanowire length increases, the nanowires begin to form microscale cavities, as mentioned earlier (Fig. 2g). Such enlarged microscale cavities open up the flow path that allows easier penetration of the mainflow directly into the cavities [25], thereby enhancing HTC. More importantly, inside these microscale cavities, it is likely that a circulating cavity flow might occur, and it is widely known that a circulating cavity flow significantly enhances HTC [26,27]. We believe that such flow penetration as well as cavity flow is the most plausible reasons for the HTC to rapidly increase again. After such HTC increase, the gradual HTC decrease can be explained by the geometry transition of the cavity. As seen from Fig. 2g, the size of the cavities tends to level off with length of the nanowires for long nanowires. This implies that the geometry of the cavity becomes deeper while the size of the cavity mouth is constant, i.e. increased cavity aspect ratio (as shown in the inset of Fig. 2g). Such transition of the geometry should make the mainflow again difficult to penetrate and weaken the cavity flow, thereby reducing HTC.

Effect of Reynolds number on HTC can be explained as follows: As mentioned earlier, there is a critical nanowire length which forms a microscale cavity having minimum size that enables mainflow penetration and initiates cavity flow. As the Reynolds number increases, the mainflow momentum increases, which should lead to the reduced critical value. This behavior is clearly seen in Fig. 5a where the critical length is reduced from 6.4 μm at Re = 10,000 to 1.4 μm at Re = 12,000 and 0.8 μm at Re = 18,000, which is indicated as red arrows. So with such a complex interaction between forced convection and microscale cavities formed by nanowires, the single-phase HTC is shown to be highly nonmonotonic.

3.3. Two-phase boiling heat transfer coefficient

Now, lets turn our interest to two-phase heat transfer. Although it is shown that the nanowires cannot enhance CHF compared to the plain surface, a large number of nucleation sites are shown to enhance HTC in nucleate boiling regime, as shown in Fig. 3. However, in the nucleate boiling regime, the results are also highly nonmonotonic.

Interesting point is that, unlike pool boiling where the phase-change is the dominant heat transfer mechanism, HTC at nucleate boiling regime is not very far from single-phase HTC. Even at CHF, the overall HTC is only about twice as much compared to the single-phase HTC, implying that the forced convection still plays a major role in the overall heat transfer at the nucleate boiling regime. This is more pronounced for the shorter nanowires where boiling is not as significant compared to the longer nanowires due to the nucleation cavity difference. Fig. 5b shows HTC vs. nanowire length at nucleate boiling regime (wall heat flux = 25 W/cm^2). It is observed that the overall trend for HTC is quite similar to the single phase HTC (Fig. 5a) at short nanowires whereas it deviates at longer nanowire. Since boiling heat transfer is more pronounced at longer nanowires due to the enlarged nucleation cavity sites [28], this implies that the forced convection is the dominant mechanism for heat transfer at shorter nanowires whereas the phase-change is dominant at longer nanowires. For instance, the longest nanowire (15.7 μm) shows the highest HTC at boiling regime despite low HTC at single-phase regime.

We can find an interesting behavior from Fig. 3d–f in terms of the slope of the curve in the nucleate boiling regime, where it represents the increment of the nucleate boiling heat transfer to the wall heat flux increase, and higher slope implies more pronounced activation of nucleate boiling. It is known that a better nucleate boiling can be achieved when the number of active nucleation sites is large [29], and the bubble departure diameter is small so that the bubble number density can be maximized [3]. From the results, it is observed that the slope varies by two distinct values, and as the nanowire length increases, the slope varies from the lower slope to higher slope, which is presented in Fig. 6. And this transition of the slope shifts from long nanowire to short nanowires as the Reynolds number increases (as marked with red arrows).

This is somewhat in conjunction with what we have observed in single-phase HTC in Fig. 5a, where the critical nanowire length required for initiating the cavity flow and mainflow penetration increases with the Reynolds number. In this regard, this implies that a strengthened mainflow momentum and the associated cavity flow/mainflow penetration has provoked more nucleation of bubbles in a way that favors boiling heat transfer since the microscale cavities that can be acted as nucleation sites are lesser at shorter nanowires. As seen from the visualization results in Fig. 7, where it shows the nucleated and departing bubbles at a moment after the ONB (onset of nucleate boiling), the overall bubble departure diameter is shown to be decreased as the Reynolds number increases, which is a direct indicative of increased active nucleation sites.

Shear between the mainflow and the bubble inside the cavity may favor easier bubble departure, enabling smaller bubble departure diameter. Also, since local pressure inside the cavity is relatively low, this will result in more enhanced penetration of the

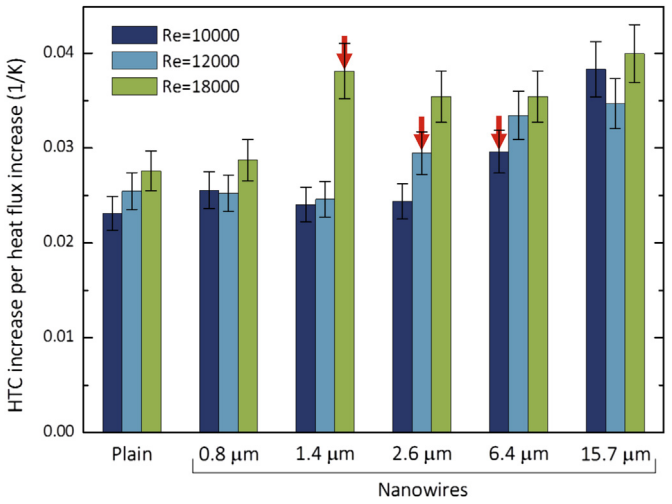

Fig. 6. Slope of the HTC vs. wall heat flux curve (HTC increase per wall heat flux increase, Fig. 2) near 25 W/cm^2 for various surfaces under different Reynolds number. Red arrows indicate minimum nanowire length for initiation of abrupt increase in the slope. (For interpretation of the references to color in this figure legend, the reader is referred to the web version of this article.)

liquid to the cavity that may favor easier bubble departure. Furthermore, flow oscillation is likely to occur near the cavity, which can induce more unstable flow that may result in easier bubble departure [30]. We believe that these are the main reasons why the slope of the heat transfer coefficient vs. heat flux increases as Reynolds number increases. Therefore, for flow boiling on a nanowire-coated surface with highly wetting fluid, the boiling behavior is shown to be highly nonmonotonic because of coupled interaction between wetting/capillary pumping, nucleation sites, and forced convection.

4. Conclusions

In summary, we have investigated flow boiling heat transfer on SiNWs-coated surfaces using highly-wetting dielectric liquid, FC-72. An unusual wetting behavior was observed for FC-72 where the presence of nanowires has reduced wettability that led to significant CHF decrease compared to the plain surface. Also, effects of the nanowire length as well as the Reynolds number on HTC were shown to be highly nonmonotonic, and we have captured several specific trends that were the keys to the complex behavior. Detailed studies should be investigated by liquids with different wettability and ordered nanowires to further elucidate the complex boiling behavior. Nevertheless, we have shown that the wetting, nucleation cavities and forced convection have participated mutually that resulted in an interesting heat transfer behavior. We conclude by emphasizing that a nanowire should not be considered as a ubiquitous medium for enhancing boiling heat transfer.

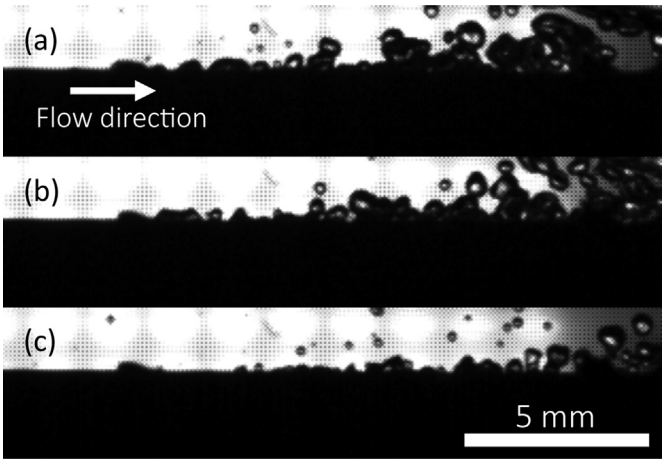

Fig. 7. Bubble images of nanowire surface (length = 1.4 μm) at a moment after ONB obtained by high-speed camera. (a) *Re* = 10,000; (b) *Re* = 12,000; (a) *Re* = 18,000.

Acknowledgments

The authors thank H. A. Stone for valuable comments and discussions. This work was supported by the National Research Foundation of Korea (NRF) under a grant funded by the Korea government (MEST) (No. 2011-0017673) and the Human Resources Development program of the Korea Institute of Energy Technology Evaluation and Planning (KETEP) under a grant funded by the Korea government Ministry of Trade, Industry and Energy (No. 20144030200560). S. Shin acknowledges the NRF for supporting through the Basic Science Research Program (No. 2013R1A6A3A03020179).

References

[1] Dhir VK. Boiling heat transfer. Ann Rev Fluid Mech 1998;30(1):365–401.
[2] Chen R, Lu M, Srinivasan V, Wang Z, Cho HH, Majumdar A. Nanowires for enhanced boiling heat transfer. Nano Lett 2009;9(2):548–53.
[3] Li C, Wang Z, Wang P, Peles Y. Nanostructured copper interfaces for enhanced boiling. Small 2008;4(8):1084–8.
[4] Ahn H, Jo H, Kang S, Kim M. Effect of liquid spreading due to nano/micro-structures on the critical heat flux during pool boiling. Appl Phys Lett 2011;98:071908.
[5] Lu M-C, Chen R, Srinivasan V, Carey VP, Majumdar A. Critical heat flux of pool boiling on Si nanowire array-coated surfaces. Int J Heat Mass Transf 2011;54:5359–67.
[6] Shin S, Kim BS, Choi G, Lee H, Cho HH. Double-templated electrodeposition: simple fabrication of micro-nano hybrid structure by electrodeposition for efficient boiling heat transfer. Appl Phys Lett 2012;101(25):251909.
[7] Kim BS, Shin S, Lee D, Choi G, Lee H, Kim KM, et al. Stable and uniform heat dissipation by nucleate-catalytic nanowires for boiling heat transfer. Int J Heat Mass Transf 2014;70:23–32.
[8] Li D, Wu G, Wang W, Wang Y, Liu D. Enhancing flow boiling heat transfer in microchannels for thermal management with monolithically-integrated silicon nanowires. Nano Lett 2012;12:3385–90.
[9] Morshed A, Yang F, Ali MY. Enhanced flow boiling in a microchannel with integration of nanowires. Appl Therm Eng 2012;32:68–75.
[10] Im Y, Joshi Y, Dietz C, Lee SS. Enhanced boiling of a dielectric liquid on copper nanowire surfaces. Int J Micro-Nano Scale Transp 2010;1(1):79–96.
[11] Mattia D, Bau H, Gogotsi Y. Wetting of CVD carbon films by polar and nonpolar liquids and implications for carbon nanopipes. Langmuir 2006;22:1789–94.
[12] 3M Fluorinert Electronic Liquid FC-72 Product Information.
[13] Huang Z, Geyer N, Werner P, de Boor J, Gosele U. Metal-assisted chemical etching of silicon: a review. Adv Mater 2011;23(2):285–308.
[14] Kim BS, Shin S, Shin SJ, Kim KM, Cho HH. Control of superhydrophilicity/superhydrophobicity using silicon nanowires via electroless etching method and fluorine carbon coatings. Langmuir 2011;27(16):10148–56.
[15] Kim BS, Shin S, Shin SJ, Kim KM, Cho HH. Micro-nano hybrid structures with manipulated wettability using a two-step silicon etching on a large area. Nanoscale Res Lett 2011;6(1):333.
[16] B. S. Kim, K. M. Yang, S. Shin, G. Choi, H. H. Cho, Local nucleation propagation on heat transfer uniformity during subcooled convective boiling, Heat Mass Transf. http://dx.doi.org/10.1007/s00231-014-1379-0.
[17] Kandlikar S. Fundamental issues related to flow boiling in minichannels and microchannels. Exp Therm Fluid Sci 2002;26:389–407.
[18] Kousalya A, Hunter C, Putnam SA, Miller T, Fisher TS. Photonically enhanced flow boiling in a channel coated with carbon nanotubes. Appl Phys Lett 2012;100:071601.
[19] Dhir VK, Liaw SP. Framework for a unified model for nucleate and transition pool boiling. J Heat Transf 1989;111(3):3739–46.
[20] Kandlikar SG. A theoretical model to predict pool boiling CHF incorporating effects of contact angle and orientation. J Heat Transf 2001;123(6):1071–9.
[21] Wenzel R. Resistance of solid surfaces to wetting by water. Ind Eng Chem 1936;28(8):988–94.
[22] Quere D. Wetting and roughness. Annu. Rev Mater Res 2008;38:71–99.
[23] Cassie A, Baxter S. Wettability of porous surfaces. Trans Faraday Soc 1944;40:546–50.

[24] Sathyamurthi V, Ahn H, Banerjee D, Lau S. Subcooled pool boiling experiments on horizontal heaters coated with carbon nanotubes. J Heat Transf 2009;131:071501.
[25] Fishler R, Mulligan MK, Sznitman J. Mapping low-Reynolds number microcavity flows using microfluidic screening devices. Microfluid. Nanofluid 2013;15:491–500.
[26] Alammar K. Effect of cavity aspect ratio on flow and heat transfer characteristics in pipes: a numerical study. Heat Mass Transf 2006;42:861–6.
[27] Ooi A, Iaccarino G, Behnia M. Heat transfer predictions in cavities. Ann Res Briefs 1998:185–96.
[28] Yao Z, Lu Y, Kandlikar S. Effects of nanowire height on pool boiling performance of water on silicon chips. Int J Therm Sci 2011;50:2084–90.
[29] Hsu YY. On the size range of active nucleation cavities on a heating surface. J Heat Transf 1962;84(3):207.
[30] Heller H, Holmes D, Covert E. Flow-induced pressure oscillations in shallow cavities. J Sound Vib 1971;18(4):545–53.